Ion-Transport Catalysis: Catalyzed Isomerizations of NNH^+ and $NNCH_3^+$

Andrew J. Chalk and Leo Radom*

Contribution from the Research School of Chemistry, Australian National University, Canberra, ACT 0200, Australia

Received August 14, 1998. Revised Manuscript Received December 1, 1998

Abstract: High-level ab initio calculations using the G2** and G2(ZPE=MP2) methods have been employed to examine the effect of interaction with a range of neutral molecules (X) on the barrier to the degenerate proton-transport reactions in NNH^+ (X = Ar, HF, CO, N_2, H_2O) and methyl cation-transport reactions in $NNCH_3^+$ (X = HF, H_2, N_2, HCl, H_2O). It is found that the barriers to both proton and methyl cation transport are lowered from their values in the isolated ions of 182 and 152 kJ mol^{-1}, respectively, by interaction with species having values of the proton or methyl cation affinity, respectively, lower than that of molecular nitrogen. Interaction with species that have larger values of proton or methyl cation affinities leads to a further lowering of the barrier, but transfer to the neutral molecule X becomes the more energetically favorable process in such cases. It is found that the ideal catalyst for ion transport should have an ion affinity close to but less than that of molecular nitrogen and have a large dipole moment.

Introduction

There have been many examples in the recent literature[1−4] of the phenomenon described by Bohme[4] as proton-transport catalysis, namely the lowering or even elimination of the barrier to a proton-transport reaction that occurs in the presence of a neutral base. However, few examples of catalysis of other ion-transport reactions have been reported. The only experimental study of which we are aware involves the isomerization of $CH_3NO_2^+$ to CH_3ONO^+, which was found to be catalyzed by both nitrogen and xenon.[5] Theoretical work on the isomerization of CH_3OC^+ to $OCCH_3^+$, which found a lowering of the barrier to methyl cation migration by interaction with nitrogen and argon, has also been reported.[3]

In recent systematic studies, we found that the proton affinity of the added neutral molecule plays a crucial role in determining its effectiveness as a proton-transport catalyst.[2] It was concluded that the ideal catalyst should have a proton affinity lying between those of the two sites between which the proton is migrating.[2,4] In the case of degenerate rearrangements such as those that might occur in NNH^+, the two sites are the same, so this condition cannot be satisfied. A study of such a system has not yet been reported.

A suggestion that the methyl cation affinity of a neutral is important in determining its effectiveness as a methyl cation-transport catalyst has also been made.[5] The proposed mechanism for methyl cation transport, however, differs from that for proton transport due to the barrier that will generally exist for transfer of a methyl cation between the two species within the initially formed complex **a**, as shown in Scheme 1.[5]

The present work aims first to systematically investigate the possibility of catalysis of proton-transport reactions in a degenerate system and second to make comparisons between proton transport and the corresponding methyl cation-transport reaction. This includes a detailed investigation of the mechanism for methyl cation-transport catalysis (Scheme 1). Results are reported for the isomerization of the isolated NNH^+ and $NNCH_3^+$ systems and for proton transport and methyl cation transport catalyzed by a range of neutral molecules (Ar, HF, CO, N_2, H_2O; or HF, H_2, N_2, HCl, H_2O).

Methods and Results

Standard ab initio molecular orbital calculations[6] have been carried out with the GAUSSIAN 94[7] and MOLPRO[8] programs

(1) See, for example: (a) Nobes, R. H.; Radom, L. *Chem. Phys.* **1981**, *60*, 1. (b) Wagner-Redeker, W.; Kemper, P. R.; Jarrold, M. F.; Bowers, M. T. *J. Chem. Phys.* **1985**, *83*, 1121. (c) Freeman, C. G.; Knight, J. S.; Love, J. G.; McEwan, M. J. *Int. J. Mass Spectrom. Ion Processes* **1987**, *80*, 255. (d) Ferguson, E. E. *Chem. Phys. Lett.* **1989**, *156*, 319. (e) Petrie, S.; Freeman, C. G.; Meot-Ner, M.; McEwan, M. J.; Ferguson, E. E. *J. Am. Chem. Soc.* **1990**, *112*, 7121. (f) Bosch, E.; Lluch, J. M.; Bertran, J. *J. Am. Chem. Soc.* **1990**, *112*, 3868. (g) Petrie, S.; Freeman, C. G.; Meot-Ner, M.; McEwan, M. J.; Ferguson, E. E. *J. Am. Chem. Soc.* **1990**, *112*, 7121. (h) Fox, A.; Bohme, D. K. *Chem. Phys. Lett.* **1991**, *187*, 541. (i) Audier, H. E.; Millet, A.; Leblanc, D.; Morton, T. H. *J. Am. Chem. Soc.* **1992**, *114*, 2020. (j) Ruttink, P. J. A.; Burgers, P. C. *Org. Mass Spectrom.* **1993**, *28*, 1087. (k) Mourgues, P.; Audier, H. E.; Leblanc, D.; Hammerum, S. *Org. Mass. Spectrom.* **1993**, *28*, 1098. (l) Becker, H.; Schröder, D.; Zummack, W.; Schwarz, H. *J. Am. Chem. Soc.* **1994**, *116*, 1096. (m) Audier, H. E.; Leblanc, D.; Mourgues, P.; McMahon, T. B.; Hammerum, S. *J. Chem. Soc., Chem. Commun.* **1994**, 2329. (n) Chou, P. K.; Smith, R. L.; Chyall, L. J.; Kenttämaa, H. I. *J. Am. Chem. Soc.* **1995**, *117*, 4374, 9831. (o) Gauld, J. W.; Audier, H.; Fossey, J.; Radom, L. *J. Am. Chem. Soc.* **1996**, *118*, 6299. (p) Ruttink, P. J. A.; Burgers, P. C.; Terlouw, J. K. *Can. J. Chem.* **1996**, *74*, 1078.

(2) (a) Chalk, A. J.; Radom, L. *J. Am. Chem. Soc.* **1997**, *119*, 7573. (b) Gauld, J. W.; Radom, L. *J. Am. Chem. Soc.* **1997**, *119*, 9831.

(3) Cunje, A.; Rodriquez, C. F.; Bohme, D. K.; Hopkinson, A. C. *J. Phys. Chem. A* **1998**, *102*, 478.

(4) Bohme, D. K. *Int. J. Mass Spectrom. Ion Processes* **1992**, *115*, 95.

(5) Baranov, V.; Petrie, S.; Bohme, D. K. *J. Am. Chem. Soc.* **1996**, *118*, 4500.

(6) Hehre, W. J.; Radom, L.; Schleyer, P. v. R.; Pople, J. A. *Ab Initio Molecular Orbital Theory*; Wiley: New York, 1986.

(7) Frisch, M. J.; Trucks, G. W.; Schlegel, H. B.; Gill, P. M. W.; Johnson, B. G.; Robb, M. A.; Cheeseman, J. R.; Keith, T. A.; Petersson, G. A.; Montgomery, J. A.; Raghavachari, K.; Al-Laham, M. A.; Zakrzewski, V. G.; Ortiz, J. V.; Foresman, J. B.; Cioslowski, J.; Stefanov, B. B.; Nanayakkara, A.; Challacombe, M.; Peng, C. Y.; Ayala, P. Y.; Chen, W.; Wong, M. W.; Andres, J. L.; Replogle, E. S.; Gomperts, R.; Martin, R. L.; Fox, D. J.; Binkley, J. S.; Defrees, D. J.; Baker, J.; Stewart, J. P. P.; Head-Gordon, M.; Gonzalez, C.; Pople, J. A. *GAUSSIAN 94*, Revision D.1; Gaussian Inc.; Pittsburgh, PA, 1995.

10.1021/ja982928l CCC: $18.00
Published on Web 02/04/1999

Scheme 1

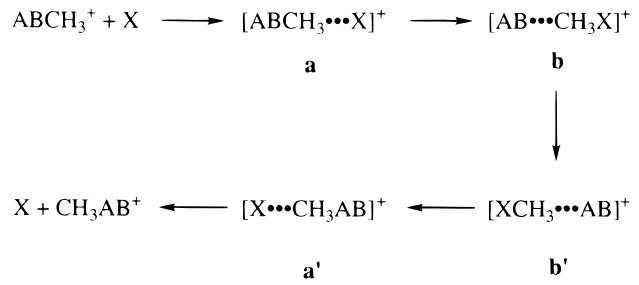

using variants of the G2 method.[9] The G2 procedure has been shown to perform well in the prediction of a number of thermochemical quantities,[10] including proton affinities[11] and methyl cation affinities.[12] The G2 level of theory corresponds effectively to QCISD(T)/6-311+G(3df,2p) energies at MP2/6-31G(d) optimized geometries with the addition of zero-point vibrational energy (ZPVE) and a so-called higher level correction. To provide a better description of the hydrogens in the proton-transport reactions, polarization functions have been included (i.e., 6-31G(d,p) rather than 6-31G(d) in the geometry optimizations and ZPVE) in the calculations for these systems. In addition, ZPVE calculations have been performed at the MP2 level (and scaled by 0.9427) rather than HF. We term this level of theory G2**. The methyl cation-transport systems have been examined using standard G2(ZPE=MP2) theory.[13]

Calculated G2** and G2(ZPE=MP2) energies for the proton- and methyl cation-transport systems, respectively, are presented in Tables S1 and S2 of the Supporting Information. Selected geometrical features are given in Figures 1−4, while complete geometries are given in the form of GAUSSIAN archive files in Tables S3 and S4 of the Supporting Information. Unless otherwise noted, relative energies within the text refer to G2** (proton-transport systems) or G2(ZPE=MP2) (methyl cation-transport systems) values.

Discussion

Rearrangement of the Isolated NNH^+ Cation. The potential energy profile for the degenerate rearrangement of NNH^+ (**1**) via the transition structure **TS:1→1′** is shown in Figure 5. A significant barrier (182 kJ mol^{-1}) is found to exist for this process at the G2** level.

Interaction of NNH^+ with Ar. Interaction of NNH^+ with argon leads initially to the ion−neutral complex **2**, which is stabilized by 31 kJ mol^{-1} relative to the isolated species (Figure 5). A stronger interaction (72 kJ mol^{-1}) occurs with the transition structure **TS:2→2′** to form the rearranged product **2′**, resulting in a reduction in the overall barrier from 182 to 110 kJ mol^{-1}.

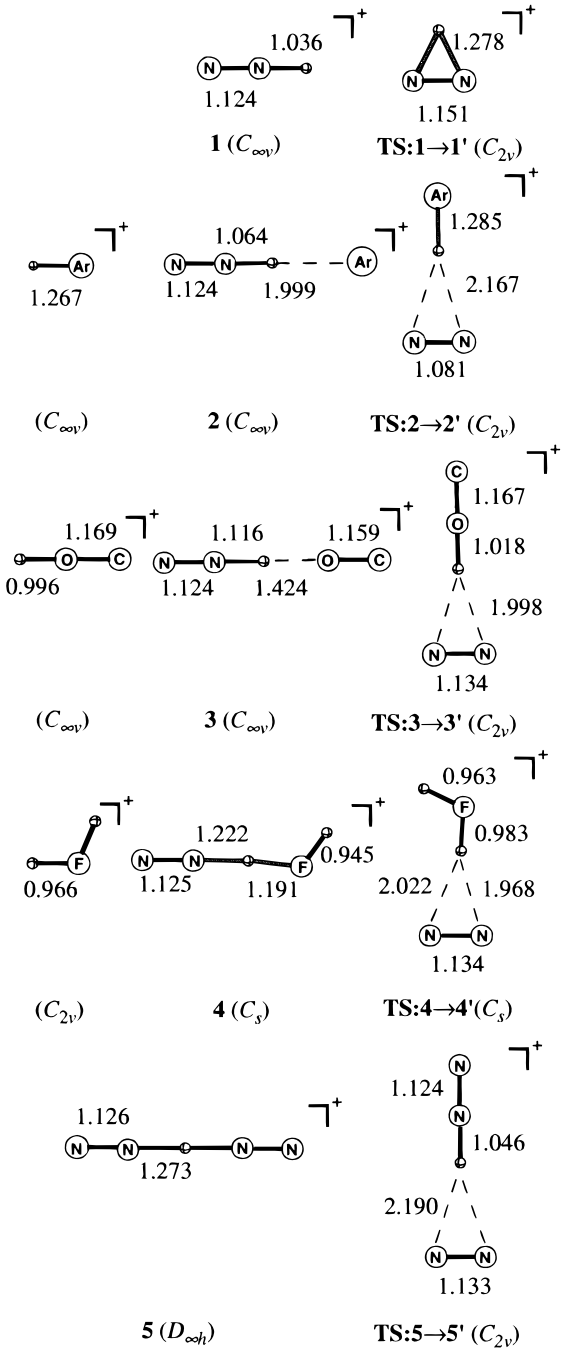

Figure 1. Selected MP2/6-31G(d,p) geometrical parameters for the isolated NNH^+ and HX^+ structures, and for the $[NNH\cdots X]^+$ structures with X = Ar, HF, CO*, and N_2.

Interaction of NNH^+ with CO (at O), HF, and N_2. As the proton affinity of the interacting neutral molecule is increased (Table 1), we find a corresponding increase in the interaction energies and a decrease in the barrier to hydrogen migration (Figure 5), consistent with previous work.[2,3] The overall barrier decreases from its value of 182 kJ mol^{-1} in the isolated case to 40 kJ mol^{-1} in the presence of CO* (protonating at oxygen), −13 kJ mol^{-1} in the presence of HF, and −12 kJ mol^{-1} in the presence of N_2.

Interaction of NNH^+ with CO (at C) and H_2O. The molecules *CO (protonating at carbon) and H_2O have proton

(8) MOLPRO is a package of ab initio programs written by H. J. Werner and P. J. Knowles with contributions from J. Almlof, R. D. Amos, M. J. O. Deegan, S. T. Elbert, C. Hampel, W. Meyer, K. Peterson, R. Pitzer, A. J. Stone, P. R. Taylor, and R. Lindh.

(9) Curtiss, L. A.; Raghavachari, K.; Trucks, G. W.; Pople, J. A. *J. Chem. Phys.* **1991**, *94*, 7221.

(10) For recent reviews on G2 theory, see: (a) Curtiss, L. A.; Raghavachari, K. In *Quantum Mechanical Electronic Structure Calculations with Chemical Accuracy*; Langhoff, S. R., Ed.; Kluwer Academic Publishers: Dordrecht, The Netherlands, 1995. (b) Raghavachari, K.; Curtiss, L. A. In *Modern Electronic Structure Theory*; Yarkony, D. R., Ed.; World Scientific: Singapore, 1995.

(11) Smith, B. J.; Radom, L. *J. Am. Chem. Soc.* **1993**, *115*, 4885.

(12) Glukhovstev, M. N.; Szulejko, J. E.; McMahon, T. B.; Gauld, J. W.; Scott, A. P.; Smith, B. J.; Pross, A.; Radom, L. *J. Phys. Chem.* **1994**, *98*, 13099.

(13) Curtiss, L. A.; Raghavachari, K.; Pople, J. A. *J. Chem. Phys.* **1995**, *103*, 4192.

(14) Lias, S. G.; Bartmess, J. E.; Liebman, J. F.; Holmes, J. L.; Levin, R. D.; Mallard, W. G. *J. Phys. Chem. Ref. Data Suppl.* **1988**, *17*.

(15) Szulejko, J. E.; McMahon, T. B. *J. Am. Chem. Soc.* **1993**, *115*, 7839.

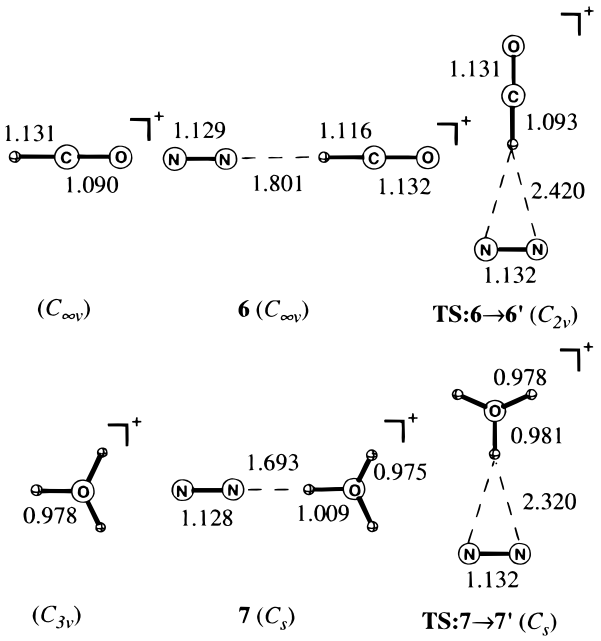

Figure 2. Selected MP2/6-31G(d,p) geometrical parameters for the HX^+ and $[NNH\cdots X]^+$ structures with X = *CO and H_2O.

affinities greater than that of nitrogen (Table 1). Interaction with these species results in a further lowering of the overall barriers to −105 kJ mol^{-1} (*CO) and −200 kJ mol^{-1} (H_2O) (Figure 6). However, the fact that these two species have proton affinities greater than that of nitrogen means that it is energetically more favorable for the neutral to retain the proton than for proton migration to occur; i.e., the protonated neutral molecule plus nitrogen will be the energetically favored products in such situations (Figure 6).

Role of Proton Affinities. In previous work on the catalyzed isomerization of HOC^+ to OCH^+, we found a direct correlation of the overall barrier with the proton affinity of the neutral X and also with the H−O bond length in the initially formed complex.[2a] Similar behavior is observed here for NNH^+ (Table 2). There is generally a steady decrease in the barrier from the value of 182 kJ mol^{-1} in the isolated system to −200 kJ mol^{-1} in the presence of water. A corresponding increase in the N−H bond length with increasing proton affinity of the neutral is also observed, consistent with a weakening by interaction with X of the N−H bond, thus allowing isomerization to occur more readily. There is also a stronger interaction in the transition structure than in the complex in all cases because the weaker bonds in the transition structure allow greater interaction with the neutral, as observed previously.[2a]

Rearrangement of the Isolated $NNCH_3^+$ Cation. The potential energy profile for methyl cation migration in the isolated $NNCH_3^+$ ion (**8**) via the transition structure **TS:8→8′** is shown in Figure 7. There is a substantial barrier of 152 kJ mol^{-1} at the G2(ZPE=MP2) level.

Interaction of $NNCH_3^+$ with HF. The potential energy profile showing the effect of interaction of $NNCH_3^+$ with HF, the species with the lowest methyl cation affinity among those studied (Table 3), is included in Figure 7. The initially formed complex **9a**, which is best described as $[NNCH_3\cdots FH]^+$, is stabilized by 35 kJ mol^{-1} relative to HF plus $NNCH_3^+$. Ion **9a** can undergo a methyl cation shift to form a new complex (**9b**) via the transition structure **TS:9a→9b**, which lies at 38 kJ mol^{-1}. Complex **9b** is best described as $[NN\cdots CH_3FH]^+$ and has a relative energy of 41 kJ mol^{-1}. This energy is actually slightly higher than that of the transition structure **TS:9a→9b** after the inclusion of ZPVE, making it likely that **9b** lies at best in a very shallow potential energy well. The components of **9b** are relatively free to undergo mutual rotation. This is reflected in the transition structure **TS:9b→9b′** for the methyl cation migration that leads to the equivalent complex $[HFCH_3\cdots NN]^+$ (**9b′**) having a relative energy of just 55 kJ mol^{-1}, only 14 kJ mol^{-1} above complex **9b**. Continuation via **TS:9b′→9a′** and complex **9a′** gives the desired rearranged product, CH_3NN^+ (**8′**). The overall barrier for this process is 55 kJ mol^{-1}, a reduction of 97 kJ mol^{-1} from that in the isolated system.

Interaction of $NNCH_3^+$ with H_2 and N_2. Both H_2 and N_2 have methyl cation affinities higher than that of HF (Table 3), and it would therefore be expected that interaction with these molecules would result in a greater lowering of the overall barrier. The barriers for the methyl cation migration step do indeed drop substantially, as reflected in the relative energy of the appropriate transition structure, **TS:b→b′**, for these processes which falls from 152 to 4 kJ mol^{-1} in the presence of hydrogen and −7 kJ mol^{-1} in the presence of nitrogen (Figure 7). However, the rate-limiting step for methyl cation transport in these cases is the transformation of the $[NNCH_3\cdots X]^+$ complex (**a**) to the $[NN\cdots CH_3X]^+$ complex (**b**). The barriers to this transformation involving hydrogen (relative energy of 73 kJ mol^{-1}) and nitrogen (relative energy of 45 kJ mol^{-1}) are quite large. Hence, the overall barriers are reduced but to a smaller extent than might otherwise be suggested, namely from 152 to 73 kJ mol^{-1} in the presence of hydrogen and to 45 kJ mol^{-1} in the presence of nitrogen.

Interaction of $NNCH_3^+$ with HCl and H_2O. Hydrogen chloride and water have methyl cation affinities larger than nitrogen (Table 3), and we would therefore expect interaction with these molecules to lead to a further lowering of the barriers for methyl cation migration. This is indeed the case, the overall barriers being reduced from 152 to 26 and −12 kJ mol^{-1}, respectively (Figure 8). Again, the methyl cation transfer in the complex between N_2 and X (via **TS:a→b**) is the rate-limiting step. As for the analogous case in proton transfer, the fact that the neutral has a higher methyl cation affinity than nitrogen means that the favored products will be XCH_3^+ plus N_2 rather than the desired isomerized product, CH_3NN^+ (**8′**).

Other Reactions. In species where the neutral X contains a proton (i.e., the neutral can be described as HZ with Z = F, H, Cl, or OH), there is the possibility of an additional reaction that has not been discussed above, namely proton transfer from CH_3ZH^+ to nitrogen. The reaction energies for the production of protonated nitrogen plus CH_3Z are 161 (Z = F), 56 (Z = H), 136 (Z = Cl), and 164 (Z = OH) kJ mol^{-1}. Apart from the case of Z = H (i.e., X = H_2), all these energies are significantly higher than that of the rate-limiting step for formation of isomerized $NNCH_3^+$ and hence such proton-transfer will not be energetically favorable. In the case of X = H_2, however, we would expect some formation of CH_4 plus NNH^+ because the energy required to form these species (56 kJ mol^{-1}) is less than the energy of the rate-limiting step for isomerization of $NNCH_3^+$ (73 kJ mol^{-1}). CH_4 and NNH^+ are formed from **10b**, initially via the transition structure **TS:10b→10c** at −9 kJ mol^{-1}. The latter is lower in energy than the resulting complex (**10c**) at 3 kJ mol^{-1}, indicating a very flat potential for proton transfer. Dissociation of **10c** then results in CH_4 plus NNH^+ at an energy of 56 kJ mol^{-1}.

For the reactions of $NNCH_3^+$ with H_2, there is also the possibility of exchange of labeled hydrogens within complex **10b**. Recent work has shown that the CH_5^+ ion has very low

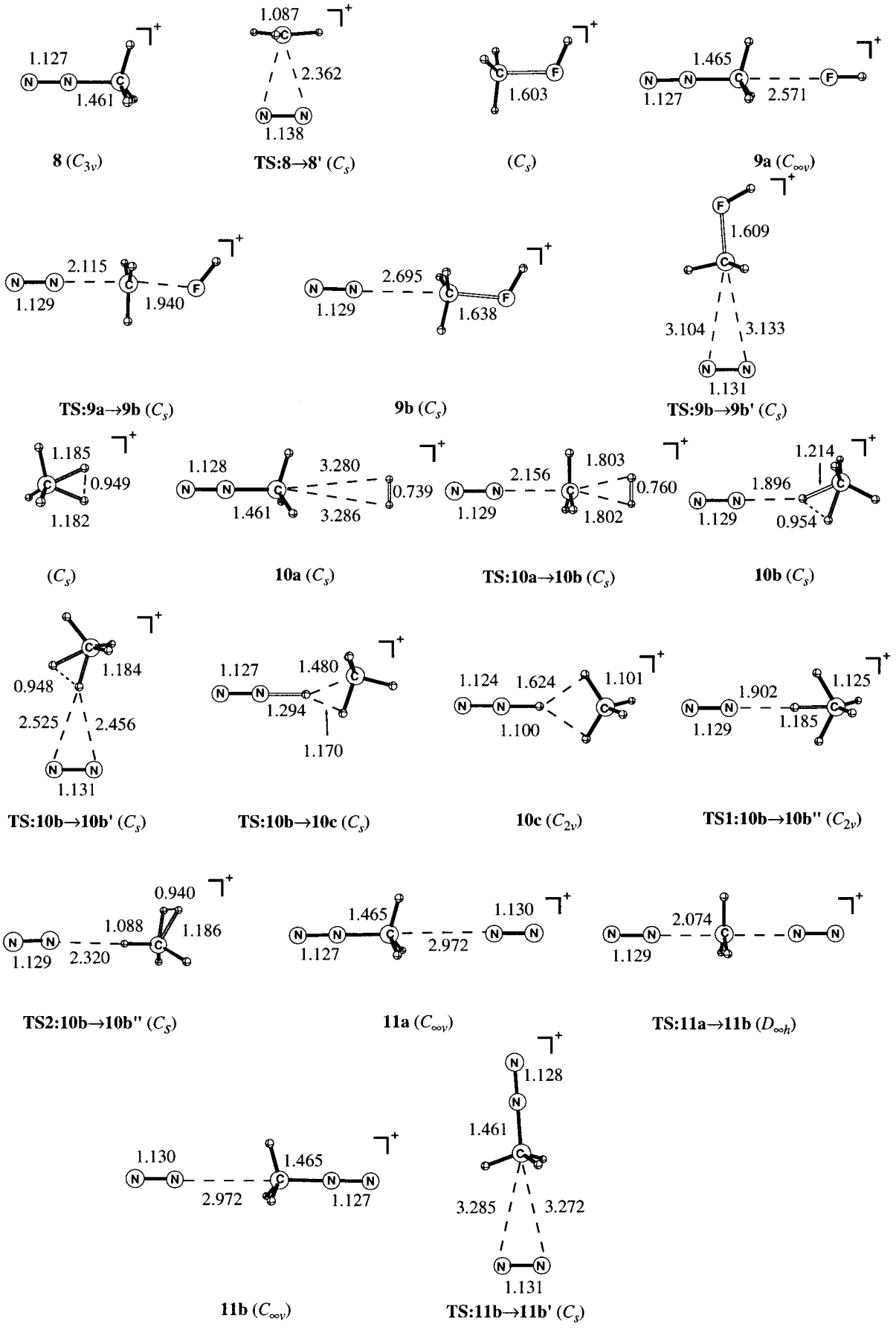

Figure 3. Selected MP2/6-31G(d) geometrical parameters for the isolated $NNCH_3^+$ and CH_3X^+ structures, and for the $[NNCH_3\cdots X]^+$ structures with X = HF, H_2, and N_2.

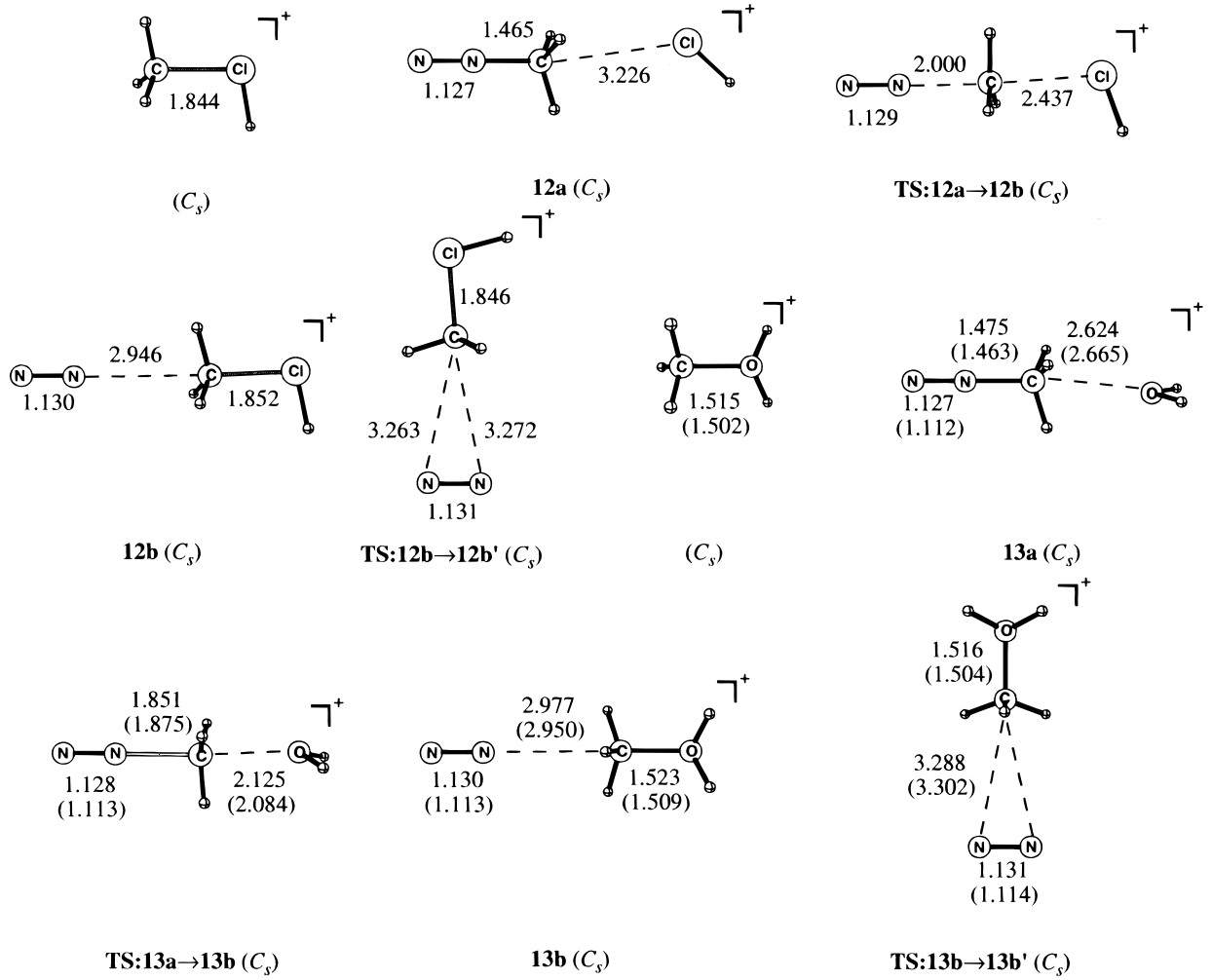

Figure 4. Selected MP2/6-31G(d) and MP2/6-311+G(3df,2p) (in parentheses) geometrical parameters for the CH_3X^+ and $[NNCH_3\cdots X]^+$ structures with X = HCl and H_2O.

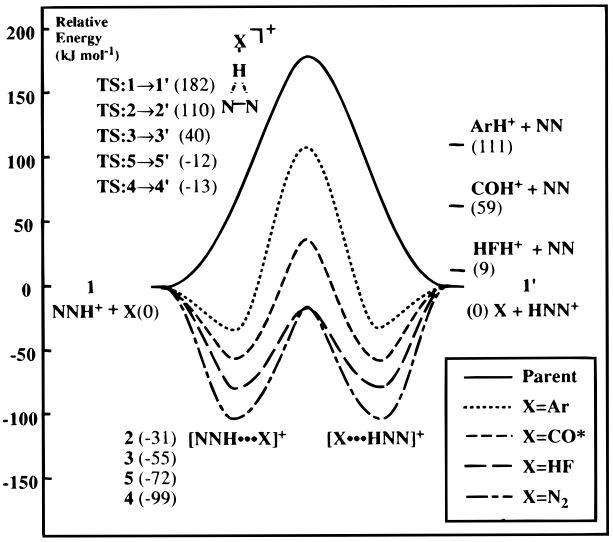

Figure 5. Schematic energy profile (G2**, 0 K) showing the uncatalyzed (parent) and catalyzed (X = Ar, HF, CO*, N_2) isomerization of NNH^+.

barriers to internal hydrogen motions,[16] and due to the weak nature of its bonding, we would expect this property to be also exhibited in complex **10b**. We have located two transition structures (Figure 3) corresponding to hydrogen exchange within **10b**. The first, **TS1:10b→10b″** at an energy of −22 kJ mol^{-1}, results in loss of identity of the three in-plane hydrogens. This energy is actually lower than that of complex **10b**, indicating an extremely flat potential surface for such a motion. A second transition structure (**TS2:10b→10b″**) at a relative energy of −3 kJ mol^{-1} will result in exchange of in-plane with out-of-plane hydrogens. Since the energies of both these transition structures lie below the energy of the separated species, we would expect a total loss of identity of all hydrogen labels. This would mean that in the proton-transfer reaction discussed above, the transferred hydrogen should be chosen randomly from the five available hydrogens.

Table 1. Calculated and Experimental Proton Affinities

species	G2** 0 K	G2** 298 K	expt[a] 298 K
Ar	377.8	381.6	371
CO*	430.1	433.5	427[b]
HF	480.3	485.3	489.5
N_2	488.9	494.4	494.5, 496.5[c]
*CO	588.2	593.9	594, 593.6[c]
H_2O	682.3	688.3	697, 690.2[c]

[a] From ref 14 unless otherwise noted. [b] From ref 1c. [c] From ref 15.

Mechanism for Methyl Cation-Transport. As noted above, the methyl cation-transport process actually takes place in three

(16) See, for example: (a) Schreiner, P. R.; Kim, S− J.; Schaefer, H. F.; Schleyer, P. v. R. *J. Chem. Phys.* **1993**, *99*, 3716. (b) Müller, H.; Kutzelnigg, W.; Noga, J.; Klopper, W. *J. Chem. Phys.* **1997**, *106*, 1863.

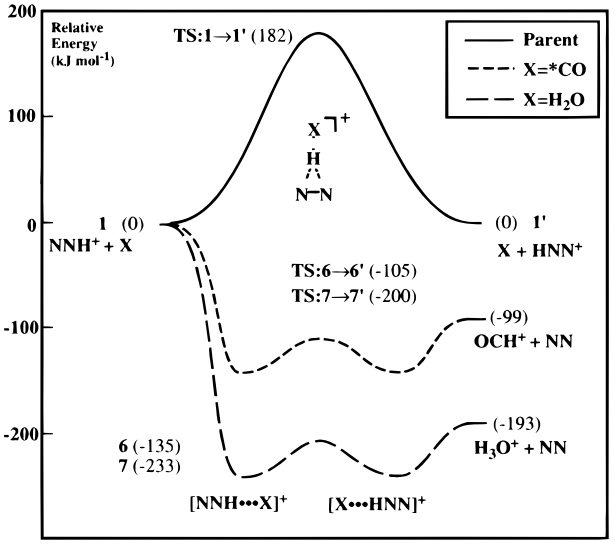

Figure 6. Schematic energy profile (G2**, 0 K) showing the uncatalyzed (parent) and catalyzed (X = *CO, H_2O) isomerization of NNH^+.

Table 2. Relative Proton Affinities (ΔPA, kJ mol^{-1}),[a,b] N···H Bond Lengths in $[NN\cdots H\cdots X]^+$ Complexes (Å),[c] and Overall Reaction Barriers (kJ mol^{-1})[b,d]

X	ΔPA	*r*(N···H)	barrier
		1.036	182
Ar	−111	1.064	110
CO*	−59	1.116	40
HF	−9	1.222	−13
N_2	0	1.273	−12
OC*	99	1.801	−105
H_2O	193	1.693	−200

[a] ΔPA = PA(X) − PA(N_2). [b] G2** at 0 K. [c] MP2/6-31G(d,p) optimized geometries. [d] Barriers relative to reactants NNH^+ + X.

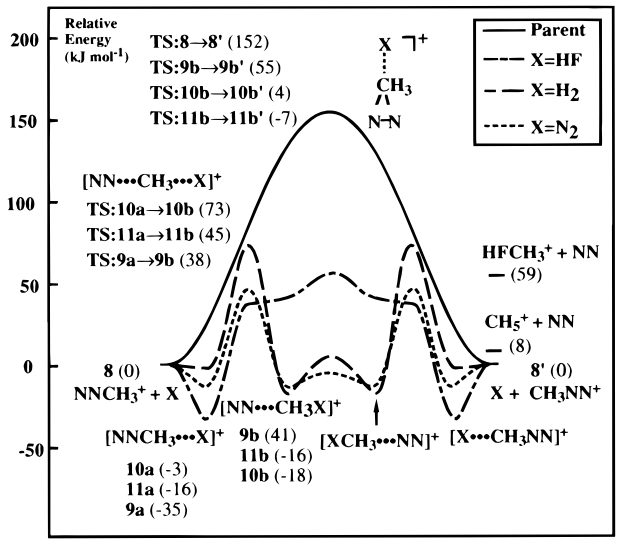

Figure 7. Schematic energy profile (G2(ZPE=MP2), 0 K) showing the uncatalyzed (parent) and catalyzed (X = HF, H_2, N_2) isomerization of $NNCH_3^+$.

steps. First, the initially formed complex $[NNCH_3\cdots X]^+$ (**a**) is converted to the alternative complex $[NN\cdots CH_3X]^+$ (**b**). The two components in the latter are fairly weakly bound, and so transformation to $[XCH_3\cdots NN]^+$ (**b′**) can occur with a low barrier, as suggested in Scheme 1. Transformation to the product-related complex $[X\cdots CH_3NN]^+$ (**a′**) takes place in the third step. In all but one of the cases examined here, the first

Table 3. Calculated and Experimental Methyl Cation Affinities

species	MP2[a,b] 0 K	MP2[b,c] 0 K	G2(MP2=ZPE) 0 K	G2(MP2=ZPE) 298 K	expt[d] 298 K
HF		149.2	114.5	120.9	134.9
H_2		139.3	165.3	173.6	188[e]
N_2	182.9	176.6	173.1	179.4	184.2
HCl		183.9	191.7	198.1	203.6
H_2O	275.4	299.2	265.0	272.9	283.3

[a] Calculated using the 6-311+G(3df,2p) basis set. [b] Includes MP2/6-31G(d) ZPVE. [c] Calculated using the 6-31G(d) basis set. [d] From ref 12 unless otherwise noted. [e] From ref 14.

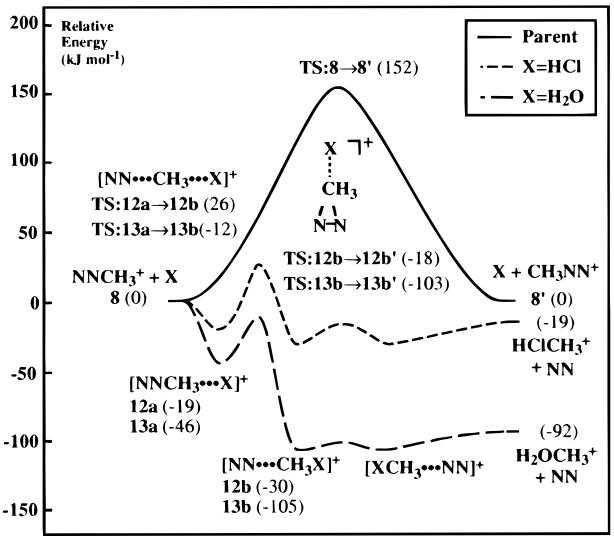

Figure 8. Schematic energy profile (G2(ZPE=MP2), 0 K) showing the uncatalyzed (parent) and catalyzed (X = HCl, and H_2O) isomerization of $NNCH_3^+$.

methyl cation transfer between the complexes (via **TS:a→b**) is the rate-determining step for the reaction; hence, for effective catalysis to occur, we would require this barrier to be low or negative. This can certainly be achieved if the reaction is sufficiently exothermic, e.g. transfer from molecular nitrogen to water (Figure 8). Unfortunately, for a neutral X to be useful in our situation, it must have a methyl cation affinity *lower* than that of nitrogen so that methyl cation migration rather than methyl cation transfer to the neutral molecule X takes place. However, this makes the methyl cation-transfer reaction (**a→b**) endothermic. Thus, it would seem that it is not feasible to eliminate the barrier entirely in such degenerate methyl cation-transport reactions, in contrast to the situation for proton transport.

Importance of Dipole Moments. Proton affinities are clearly important in determining the effectiveness of a proton-transport catalyst, but our calculations indicate that there are other factors to consider. For example, since nitrogen has a higher proton affinity than hydrogen fluoride (Table 1), we would expect, on the basis of proton affinities alone, that nitrogen would have a larger interaction with NNH^+ than hydrogen fluoride. In fact the opposite is observed. Nitrogen is found to have a significantly weaker interaction with NNH^+ (72 kJ mol^{-1}) than does hydrogen fluoride (99 kJ mol^{-1}). We believe that the stabilizing effect of ion−dipole interactions contributes to such apparent discrepancies. Thus the ion−dipole interaction of NNH^+ with hydrogen fluoride, which has a significant dipole moment (2.0 D), is greater than that with nitrogen, which has a zero dipole moment. This effect is also evident in the reaction barriers. The barrier in the presence of hydrogen fluoride (−13 kJ mol^{-1}) is

Table 4. Relative Methyl Cation Affinities (ΔMCA, kJ mol^{-1}),[a,b] Dipole Moments (D) of X,[c] N···C Bond Lengths in [NNCH$_3$···X]$^+$ (**a**) and [NN···CH$_3$X]$^+$ (**b**) Complexes (Å),[c] Stabilization Energies of [NNCH$_3$···X]$^+$ (**a**)[d] and [NN···CH$_3$X]$^+$ (**b**)[e] (E_{stab}, kJ mol^{-1}),[b] and Overall Reaction Barriers (kJ mol^{-1})[b,d]

			r(N−C)		E_{stab}		
X	ΔMCA	dipole moment	[NNCH$_3$··· X]$^+$	[NN··· CH$_3$X]$^+$	[NNCH$_3$··· X]$^+$	[NN··· CH$_3$X]$^+$	overall barrier
			1.461				152
HF	−59	2.01	1.465	2.695	35	18	55
H_2	−8	0.0	1.461	3.054	3	24	73
N_2	0	0.0	1.465	2.972	16	18	45
HCl	19	1.51	1.465	2.946	19	11	26
H_2O	92	2.25	1.475	2.977	46	13	−12

[a] ΔMCA = MCA(X) − MCA(N_2). [b] G2(ZPE=MP2) at 0 K. [c] From MP2/6-31G(d,p) optimized geometries. [d] Relative to NNCH$_3^+$ + X. [e] Relative to NN + CH$_3$X$^+$.

very slightly lower than that observed in the presence of nitrogen (−12 kJ mol^{-1}), despite the greater proton affinity of N_2.

For proton-transport systems, we have already noted the correlation between the N−H bond lengths and the proton affinity of the interacting neutral. In contrast to this behavior, there is little correlation between the methyl cation affinity of the interacting neutral and the N−C bond lengths in complexes **a** and **b** involved in methyl cation transport. It can be seen from Table 4 that these bond lengths are fairly constant, independent of the methyl cation affinity of the neutral. This, along with the fact that the neutral component of the complex is always at a reasonably large distance (Figures 3 and 4), leads us to suggest that these complexes are largely electrostatically bound.

If the intermediate complexes are indeed largely electrostatically bound, we may expect that the dipole moment of the neutral molecule plays an important role in determining the stability of the ion−neutral complex. It can be seen from Table 4 that there does indeed appear to be a correlation between the dipole moment of the neutral and the stabilization energy of the resulting complex (**a**). For example, HF, which has a relatively high dipole moment (2.0 D), forms an initial complex (**9a**) that is stabilized by 35 kJ mol^{-1}, while H_2 with a zero dipole moment forms an initial complex (**10a**) that is stabilized by only 3 kJ mol^{-1}. N_2, which also has a zero dipole moment, forms a complex (**11a**) that is stabilized by a greater amount (16 kJ mol^{-1}) due to a combination of ion−induced-dipole and ion−quadrupole interactions.[17] The magnitudes of both the polarizabilty and quadrupole moment of nitrogen are larger than those for hydrogen, resulting in the increased stabilization of the nitrogen complex. The stabilization energies increase smoothly with increasing dipole moment so that H_2O, with a dipole moment of 2.3 D, forms a complex (**13a**) that is stabilized by 46 kJ mol^{-1}. However, for all cases except HF, the relative methyl cation affinity (ΔMCA, Table 4) also correlates reasonably well with the stabilization energy, so it is possible that ΔMCA is also important in determining the stabilization of the complex.

The overall barrier for methyl cation transport is generally given by the relative energy of **TS:a→b**. This will be influenced by the energies, relative to the starting reactants of complexes **a** and **b**, as shown schematically in Figure 9. A lowering in energy of either **a** or **b** should result in a lowering of this barrier. If electrostatic interactions are important, the stabilization energy

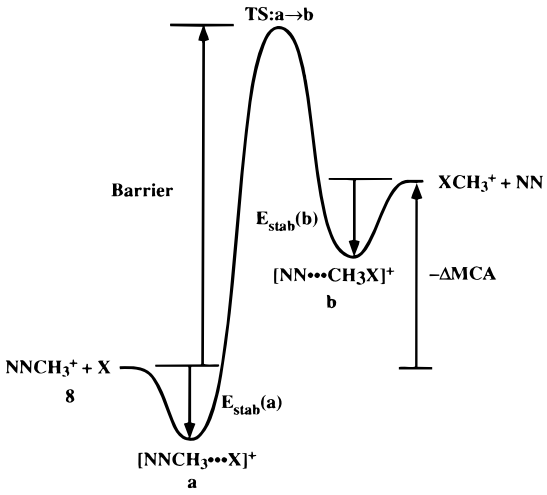

Figure 9. Schematic energy profile for methyl cation transfer (**a→b**) showing the principal factors determining the barrier height.

(E_{stab}(**a**)) of the reactant complex **a** will be increased through interaction with a neutral having a large dipole moment. The energy of the product complex **b** is affected both by E_{stab}(**b**) and by the relative methyl cation affinity (ΔMCA), which determines the relative energy of the isolated species N_2 plus CH$_3$X$^+$ (Figure 9). Hence, to lower the barrier to the reaction, we can either choose a neutral with a larger dipole moment or choose a neutral with a less negative relative methyl cation affinity (ΔMCA). It can be seen from Table 4 that an increase in the relative methyl cation affinity does indeed result in a lowering of this barrier. On the other hand, dipole effects appear to be particularly important in the case of X = HF, where the barrier is much lower than would be expected on the basis of methyl cation affinities alone. We conclude that both the methyl cation affinity and the dipole moment of the interacting neutral are important in determining its effectiveness as a catalyst for methyl cation transport. For a nonpolar neutral, the quadrupole moment and polarizability will also play a role.

Reliability of Theoretical Predictions. It is important to try to assess the reliability of the theoretical predictions made in the present work. Clearly, the ion affinities play a very important role. As noted earlier, G2 theory has been shown to perform fairly well for both proton affinities[11] and methyl cation affinities.[12] It would be expected that variants of G2 would perform equally well. It can be seen from Table 1 that there is good agreement between the G2** and the experimental proton affinities.[18] It can also be seen from Table 3 that G2(ZPE=MP2) does not perform as well in the calculation of methyl cation affinities. The mean absolute deviation between theory and experiment is 9.8 kJ mol^{-1}, with the largest deviation being 14.4 kJ mol^{-1}. We find that the G2(ZPE=MP2) methyl cation affinities are generally lower than the standard G2 results,[12] by as much as 4.1 kJ mol^{-1} for water. These lower values increase the deviation from experiment (Table 3). In the present work, methyl cation affinities relative to that of molecular nitrogen are more important than absolute methyl cation affinities. We find that the mean absolute deviation between theory and experiment for methyl cation affinities relative to nitrogen is 6.3 kJ mol^{-1}, with the largest deviation being 9.2 kJ mol^{-1}, a somewhat better result.

It is also important to examine the effect of the level of geometry optimization. The G2 methods used in the present study both use geometries optimized at the MP2 level with a relatively small basis set. It is possible that significant changes in the geometries of the complexes and transition structures and

(17) Henchman, M. In *Ion-Molecule Reactions*; Franklin, J. L., Ed.; Plenum Press: New York, 1972; Vol. I, p 192.

(18) The mean absolute deviation is 5 kJ mol^{-1} with a maximum deviation of 11 kJ mol^{-1}. The mean absolute deviation drops to 4.2 kJ mol^{-1} when more recent experimental values from ref 15 for the proton affinities of N_2, *CO, and H_2O are used.

therefore the thermochemistry could occur if this level of optimization is not adequate. Poor geometries are most likely to occur if the level of optimization does not correctly describe the relative ion affinity values. It has previously been shown that the MP2/6-31G(d,p) geometries used in the G2** method are sufficient to give good relative energies for proton-transport systems,[2a] so it only remains here to examine the situation for methyl cation transport.

The MP2/6-31G(d) methyl cation affinities are shown in Table 3. It can be seen that agreement with G2(ZPE=MP2) is poor at this level, the MP2/6-31G(d) results differing by as much as 35 kJ mol^{-1} from those of G2(ZPE=MP2). In addition, these errors vary significantly from one neutral to another, meaning that relative methyl cation affinities are also poor. On the other hand, the methyl cation affinities for N_2 and H_2O at the MP2/6-311+G(3df,2p) level agree reasonably well with the G2(ZPE=MP2) results (Table 3). More importantly, the differences from G2(ZPE=MP2) are almost the same for both molecules, meaning that their relative methyl cation affinity is also in good agreement with G2(ZPE=MP2) results. We might therefore expect the MP2/6-311+G(3df,2p) level to provide accurate geometries for the complexes and transition structures associated with the X = H_2O system, against which the MP2/6-31G(d) geometries can be assessed, particularly their effect on G2(ZPE=MP2) energies.

We have examined the effect of geometry optimizations for the case of X = H_2O. It can be seen in Figure 4 that there is little difference between the bond lengths calculated at the MP2/6-31G(d) and MP2/6-311+G(3df,2p) levels. More importantly the G2(ZPE=MP2) energies based on these new geometries for **13a** (−45.8 kJ mol^{-1}), **TS:13a→13b** (−11.3 kJ mol^{-1}), **13b** (−105.8 kJ mol^{-1}), and **TS:13b→13b′** (−102.7 kJ mol^{-1}) are in close agreement with the standard G2(ZPE=MP2) results obtained with MP2/6-31G(d) geometries of −46.2, −11.6, −105.4, and −102.5 kJ mol^{-1}, respectively. These results indicate that MP2/6-31G(d) optimized geometries provide an adequate description for the purposes of the present work.

Concluding Remarks. There are substantial barriers to the degenerate isomerizations of both NNH^+ and $NNCH_3^+$ of 182 and 152 kJ mol^{-1}, respectively. These barriers can be lowered significantly by interaction with an appropriate neutral molecule. It is found that species with proton affinities slightly lower than that of molecular nitrogen can act to lower the barrier to proton transfer so that it becomes negative. Interaction with species having methyl cation affinities lower than that of nitrogen results in substantial lowering of the barriers to methyl cation transport, but in this case they remain positive. Interaction with species having ion affinities greater than that of nitrogen results in a further lowering of the barriers. However, transfer of either the proton or the methyl cation to the neutral molecule now becomes the energetically favored process. The magnitude of the dipole moment of the neutral is found to be important. Neutrals with high dipole moments are found to be more effective catalysts, especially for methyl cation transport.

Acknowledgment. We gratefully acknowledge generous allocations of time on the Fujitsu VPP300 and the SGI Power Challenge computers of the Australian National University Supercomputing Facility.

Supporting Information Available: G2** total energies for species related to proton transport (Table S1), G2(ZPE=MP2) total energies for species related to methyl cation transport (Table S2), GAUSSIAN 94 archive entries for the MP2/6-31G(d,p) optimized geometries of species related to proton transport (Table S3), and MP2/6-31G(d) optimized geometries of species related to methyl cation transport (Table S4). This material is available free of charge via the Internet at http://pubs.acs.org.

JA982928L